

**Manchester  
Metropolitan  
University**

---

He, Lingxiao and Khanal, Praval and Morse, Chris I and Williams, Alun and Thomis, Martine (2020) Associations of combined genetic and epigenetic scores with muscle size and muscle strength: a pilot study in older women. *Journal of Cachexia, Sarcopenia and Muscle*. ISSN 2190-5991

---

**Downloaded from:** <http://e-space.mmu.ac.uk/625818/>

**Version:** Published Version

**Publisher:** Wiley Open Access

**DOI:** <https://doi.org/10.1002/jcsm.12585>

**Usage rights:** Creative Commons: Attribution-Noncommercial-No Derivative Works 4.0

Please cite the published version

<https://e-space.mmu.ac.uk>

# Associations of combined genetic and epigenetic scores with muscle size and muscle strength: a pilot study in older women

Lingxiao He<sup>1,2</sup> , Praval Khanal<sup>1,2</sup> , Christopher I. Morse<sup>2</sup> , Alun Williams<sup>2,3</sup>  & Martine Thomis<sup>1\*</sup> 

<sup>1</sup>Department of Movement Sciences, Physical Activity, Sports & Health Research Group, KU Leuven, Leuven, Belgium, <sup>2</sup>Department of Sport and Exercise Sciences, Manchester Metropolitan University, Manchester, UK, <sup>3</sup>Institute of Sport, Exercise and Health, University College London, London, UK

## Abstract

**Background** Inter-individual variance in skeletal muscle is closely related to genetic architecture and epigenetic regulation. Studies have examined genetic and epigenetic relationships with characteristics of ageing muscle separately, while no study has combined both genetic and epigenetic profiles in ageing muscle research. The aim of this study was to evaluate the association between combined genetic and methylation scores and skeletal muscle phenotypes in older women.

**Methods** Forty-eight older Caucasian women (aged 65–79 years) were included in this study. Biceps brachii thickness and vastus lateralis anatomical cross-sectional area ( $ACSA_{VL}$ ) were measured by ultrasonography. Maximum isometric elbow flexion ( $MVC_{EF}$ ) and knee extension ( $MVC_{KE}$ ) torques were measured by a customized dynamometer. The muscle-driven genetic predisposition score ( $GPS_{SNP}$ ) was calculated based on seven muscle-related single nucleotide polymorphisms (SNPs). DNA methylation levels of whole blood samples were analysed using Infinium MethylationEPIC BeadChip arrays. The DNA methylation score was calculated as a weighted sum of methylation levels of sarcopenia-driven CpG sites ( $MS_{SAR}$ ) or an overall gene-wise methylation score ( $MS_{SNP}$ , the mean methylation level of CpG sites located in muscle-related genes). Linear regression models were built to study genetic and epigenetic associations with muscle size and strength. Three models were built with both genetic and methylation scores: (1)  $MS_{SAR} + GPS_{SNP}$ , (2)  $MS_{SNP} + GPS_{SNP}$ , and (3) gene-wise combined scores which were calculated as the ratio of the SNP score to the mean methylation level of promoters in the corresponding gene. Additional models with only a genetic or methylation score were also built. All models were adjusted for age and BMI.

**Results**  $MS_{SAR}$  was negatively associated with  $ACSA_{VL}$ ,  $MVC_{EF}$ , and  $MVC_{KE}$  and explained 10.1%, 35.5%, and 40.1% of the variance, respectively.  $MS_{SAR}$  explained more variance in these muscular phenotypes than  $GPS_{SNP}$ ,  $MS_{SNP}$ , and models including both genetic and methylation scores.  $MS_{SNP}$  and  $GPS_{SNP}$  accounted for less than 8% and 5% of the variance in all muscular phenotypes, respectively. The genotype and methylation level of *CNTF* was positively related to  $MVC_{KE}$  ( $P = 0.03$ ) and explained 12.2% of the variance. The adjusted  $R^2$  and Akaike information criterion showed that models with only a  $MS_{SAR}$  performed the best in explaining inter-individual variance in muscular phenotypes.

**Conclusions** Our results improve the understanding of inter-individual variance in muscular characteristics of older women and suggest a possible application of a sarcopenia-driven methylation score to muscle strength estimation in older women while the combination with a genetic score still needs to be further studied.

**Keywords** DNA methylation score; Genetic score; Older women; Model evaluation; Muscle size; Muscle strength

Received: 13 September 2019; Revised: 8 February 2020; Accepted: 24 February 2020

\*Correspondence to: Martine Thomis, Department of Movement Sciences, Physical Activity, Sports & Health Research Group, KU Leuven, Leuven, Belgium, Tervuursevest 101, 3001, Leuven, Belgium.

Email: martine.thomis@kuleuven.be

## Introduction

Muscle mass and strength are two crucial factors in healthy ageing.<sup>1</sup> Older people with lower muscle mass and muscle strength are more likely to have a greater loss of mobility<sup>2</sup> and an increased risk of falls.<sup>3</sup> A 10-year follow-up study by Balogun *et al.*<sup>4</sup> found that lower limb muscle mass and muscle strength in older people were positively associated with health-related quality of life.

Many heritability studies have shown a genetic contribution to body composition and muscle strength in older adults. An early twin study on postmenopausal women demonstrated that genetic characteristics account for 52%, 46%, and 30% of the variance in lean body mass, leg extensor strength, and grip strength, respectively.<sup>5</sup> An older male twin study conducted by Carmelli *et al.*<sup>6</sup> showed a decreased genetic association with handgrip strength from 35% to 22% over a 10-year ageing process while the environmental influence increased from 39% to 45%. Furthermore, multiple association studies on athletes, young, and old populations have suggested some genetic variants that are closely related to body composition and muscle performance. For example, the D allele of the *ACE* I/D polymorphism is related to higher muscle strength.<sup>7</sup> Older people with the *ACE* DD genotype tend to have greater lean body mass and knee extensor strength than II carriers.<sup>8</sup> The R allele of the *ACTN3* R/X polymorphism is also associated with greater muscle power.<sup>9</sup> Young people with the R allele had significantly higher knee strength and more type IIx fibres than those of XX genotype.<sup>10</sup> The T allele in *FTO* A/T polymorphism is predisposed to increase lean body mass and is more prevalent in elite rugby players, who rely more on appendicular lean mass for success, than other rugby athletes and non-athletes.<sup>11</sup>

To study the combined genetic association with physical phenotypes, a phenotype-driven genetic predisposition score (GPS), which is calculated by adding up the number of predisposing alleles that are positively related to the corresponding phenotype, has been introduced by Williams and Folland.<sup>12</sup> With the application of the phenotype-driven GPS, studies have been able to analyse associations between genetic architectures and physical performance based on multiple polymorphisms. Spanish athletes in endurance activities (e.g. running, road cycling, and rowing) were found with a higher endurance-driven GPS than the general population.<sup>13,14</sup> Coronary artery disease patients<sup>15</sup> and older people<sup>16</sup> with higher muscle mass/strength-driven GPS also demonstrated greater muscular improvement after resistance training.

Besides the genetic aspect, muscular phenotypes are also related to multiple external factors such as physical activity and nutrients,<sup>1</sup> which might affect muscle-related gene expression through epigenetic regulation.<sup>17,18</sup> As a link between environment and genes, an epigenetic regulation modifies gene expression through several mechanisms, among which

DNA methylation is the one that has been extensively studied. In the human genome, DNA methylation occurs almost exclusively at the 5' position of cytosine in cytosine-phosphate-guanine (CpG) dinucleotides.<sup>19</sup> Many factors such as age, lifestyle, and nutrition can trigger DNA methylation changes.<sup>20</sup> DNA methylation in gene promoters is usually associated with a repression of corresponding gene expression,<sup>21</sup> while a recent study by Jeziorska *et al.*<sup>22</sup> has suggested a positive association between the CpG island methylation in intragenic regions and transcriptional activity. Because DNA methylation is a reflection of environmental exposures and gene expression status, methylation levels of several CpG sites have been suggested as biomarkers for cancer screening<sup>23</sup> and chronological age prediction.<sup>24</sup> A BMI-related epigenetic score developed by Hamilton *et al.*<sup>25</sup> was found to be associated with body mass, aerobic capacity, type 2 diabetes, and cardiovascular disease. The accuracy and sensitivity of diagnostic<sup>26</sup> and prognostic<sup>27</sup> prediction of prostate cancer were also improved with the assistance of DNA methylation scores. Wei *et al.*<sup>28</sup> built a predictive model for clear cell renal cell carcinoma prognosis based on the methylation of five CpG sites and the model presented reliable predictions across several cohorts. Moreover, DNA methylation scores of specific CpG sites were introduced to the prediction of maternal smoking habit during pregnancy with high accuracy.<sup>29</sup>

In skeletal muscle, epigenetic regulation can be found in development and differentiation processes. The expression of genes from the myogenic regulatory factor and the myocyte enhancer factor families partly rely on DNA methylation to modify skeletal muscle proliferation and differentiation.<sup>30</sup> Meanwhile, some epigenetic traits induced by environmental stimuli can be maintained for a considerable period (e.g. 30 population doublings of cell culture,<sup>31</sup> 7 weeks of detraining<sup>32</sup>), a phenomenon known as 'epigenetic memory'.<sup>33</sup> A recent study by Seaborne *et al.*<sup>32</sup> suggested four genes (*RPL35a*, *UBR5*, *SETD3*, and *PLA2G16*) that held epigenetic memory 7 weeks after resistance training. All these four genes were characterized by a similar pattern of decreased gene expression with DNA hypermethylation during detraining and dramatically enhanced gene expression with DNA hypomethylation after retraining.<sup>32</sup> Turner *et al.*<sup>34</sup> demonstrated five genes (*FLNB*, *MYH9*, *SRGAP1*, *SRGN*, and *ZMIZ1*) with increased gene expression in the acute/chronic resistant training and retained hypomethylation status during 7 weeks of detraining, indicating an involvement of these five genes in epigenetic regulation of skeletal muscle characteristics. Lifelong regular physical activity is also associated with hypomethylated promoter regions in genes related to energy metabolism, myogenesis, and oxidative stress resistance in ageing muscle.<sup>35</sup> Notably, most methylation studies of skeletal muscle focus on identifying genes with various methylation changes under different intervention phases or between different populations, but the relationship between

methylation levels and muscular phenotypes has not been reported.

Several studies have combined genetic and epigenetic profile scores to explore hereditary and environmental associations with physical conditions such as BMI and heart disease risk. Shah *et al.* found that regression models with only BMI-derived genetic or methylation scores explained less than 10% of the inter-individual variance in BMI, while a model combining both scores improved the explained variance to 13–18%.<sup>36</sup> Another model with integrated genetic and methylation scores also outperformed (13% more accuracy) conventional risk factors in predicting coronary heart disease.<sup>37</sup> Such an approach of combined genetic and epigenetic scores suggests a new approach of studying inter-individual variance and long-term changes in muscle mass and muscle strength. A better understanding of genetic and epigenetic associations with muscular phenotypes can be beneficial to healthy ageing via improved estimation of the probability of muscle degeneration and thus prediction of frailty and sarcopenia. Therefore, our study was conducted to explore possible genetic and epigenetic connections with muscular phenotypes in a group of older women.

## Methods

### Participants

Genetic and epigenetic data of 48 older women (aged 65–79 years) were analysed in this study. These participants were conditionally selected from 247 independently living Caucasian women (aged 65–80 years) around Manchester Metropolitan University (Crewe, UK), which has been described in details in our previous paper.<sup>38</sup> Briefly, these 48 participants were generally age-matched with no muscular or nervous system problems that would affect their physical performance. With cut-off points of both skeletal muscle index (SMI) less than 6.75 kg/m<sup>2</sup><sup>39</sup> and hand grip strength (HGS) less than 26 kg (the lower quintile of HGS in all recruited 247 participants), 24 participants were classified as sarcopenic (SMI: 6.00 ± 0.47 kg/m<sup>2</sup>, HGS: 23.2 ± 2.5 kg), and the remaining 24 participants were classified as non-sarcopenic (SMI: 7.45 ± 0.67 kg/m<sup>2</sup>, HGS: 36.0 ± 3.7 kg). This study followed local ethics approval (Manchester Metropolitan University, Crewe, UK) and consent forms were signed by all participants.

### DNA extraction

A 5 mL venous blood sample was collected from each participant and stored in an EDTA-coated tube at –20°C for DNA extraction. DNA samples were extracted using a QIAcube® and QIAamp® DNA Blood Mini Kit (Qiagen,

Crawley, UK) according to the manufacturer's instructions. The extracted DNA samples were stored at –20°C for genotyping and DNA methylation analysis.

### Genotyping

Single nucleotide polymorphisms (SNPs) of seven genes were selected for genotyping. These SNPs have been reported in at least three papers as being related to muscle strength or muscle mass with a consistent direction of favourable alleles (Table S1). Duplicate genotyping was firstly made using a 192.24 Dynamic Array® IFC (Fluidigm Corp., South San Francisco, CA, US) and TaqMan SNP genotyping assays (Applied Biosystems, Paisley, UK) following the manufacturer's instructions. Briefly, a genotyping mix (4 µL) consisted of 2 µL assay loading reagent [2X] (Fluidigm), 1 µL SNP genotyping Assay Mix [40X] (Applied Biosystems), 0.2 µL ROX [50X] (Invitrogen, Carlsbad, CA, US), and 0.8 µL DNA-free water (Qiagen). A sample mix (4 µL) contained 1.6 µL DNA samples, 2.0 µL GTXpress master mix [2X] (Applied Biosystems, PN 4401892), 0.2 µL Fast GT Sample Loading Reagent [20X] (Fluidigm, PN 100–3,065), and 0.2 µL DNA-free water. All reaction mixes (7.75 µL, consisting of 3.75 µL genotyping mix and 4 µL sample mix) were loaded onto the Dynamic Array IFC following the manufacturer's instructions. The array was subsequently placed into a thermal cycler (FC1 Fluidigm, PN 100–1279 D1), and the GT 192.24 Fast v1.pcl protocol was performed. The thermal cycling protocol included an amplification at 95°C for 120 s followed by 45 cycles of denaturation for 2 s at 95°C and extension for 20 s at 60°C. Reporter dyes VIC and FAM were used for genotyping based on fluorescence detection.

About 1% of SNP-sample data points showed unsuccessful detection or inconsistent genotype results using the Fluidigm system. These SNP samples were reassessed in duplicates using a StepOnePlus Real-Time PCR system with TaqMan SNP genotyping assays and analysed using StepOnePlus analysis software (Applied Biosystems, version 2.3). The StepOnePlus reaction mix (10 µL) included 0.2 µL DNA sample, 5 µL GTXpress master mix, 4.3 µL nuclease-free water, and 0.5 µL TaqMan SNP genotyping assay [20X]. Each reaction mix was amplified for 20 s at 95°C, followed by 50 cycles of denaturation for 3 s at 95°C and extension for 20 s at 60°C. Genotypes were identified based on fluorescence detection of reporter dyes (VIC and FAM).

### DNA methylation analysis

DNA methylation was measured using Illumina® Infinium MethylationEPIC BeadChip arrays (Illumina Inc., San Diego, CA, US) at the Genomics Core facility (Center for Human Genetics, UZ/KU Leuven, Leuven, Belgium). Methylation

signal data were read by R 'Minfi' package,<sup>40</sup> background signals were corrected by normal-exponential out-of-band ('Noob') method, and methylation levels (defined as  $\beta$  values, methylation percentages at measured probes) were normalized for blood cell composition by R 'FlowSorted.Blood.EPIC' package. CpG sites were removed from the initial measurement under the following conditions: (i) with a low detection rate ( $P > 0.01$  compared with background signal); (ii) containing SNPs at the CpG interrogation or at the single nucleotide extension as suggested in the 'Minfi' package (reference array: 'Illumina Human Methylation EPIC', annotated by 'ilm10b4.hg19'); (iii) with cross-reactivity reported in the first supplementary table of Pidsley's study.<sup>41</sup> A final 788 074 CpGs were kept for further analysis.

## Muscular parameters

### Biceps brachii thickness

B-mode ultrasonography (7.5 MHz, linear array probe, 38 mm probe length, MyLab®Twice Esaote, Genoa, Italy) was used to measure biceps brachii (BB) thickness ( $THK_{BB}$ ) on the dominant side (Figure S1a). Participants sat with elbows extended and relaxed. Sagittal plane scans were taken and muscle thickness measured at three sites: 60% of the length from the acromion process of the scapula to the lateral epicondyle of the humerus<sup>42</sup> and the upper and lower sites 1 cm away from the 60% length site. Muscle thickness was measured using an image processing program (ImageJ, NIH) by the same investigator [intraclass correlation coefficient (ICC) = 0.98, based on duplicate measurements of six participants. The interrater reliability was based on a single scan assessed on two occasions. The following ICC tests were all based on the same participants]. The mean muscle thickness of the three sites was recorded as  $THK_{BB}$ .

### Vastus lateralis anatomical cross-sectional area

With participants in a standing position, the vastus lateralis (VL) origin and insertion were identified at the proximal and distal myotendinous junction under the previously mentioned ultrasound. The VL anatomical cross-sectional area ( $ACSA_{VL}$ ) was measured using an ultrasonography method developed by Reeves *et al.*<sup>43</sup> with a high reliability and validity compared with magnetic resonance imaging. In brief, participants sat while axial plane scans were taken at 50% muscle length of the VL and recorded in real time, with the ultrasound probe passing over echo-absorptive markers placed over the skin of the VL (as described by Reeves<sup>43</sup>). The acquired images were combined for  $ACSA_{VL}$  measurement (Figure S1b). The  $ACSA_{VL}$  was measured three times using ImageJ, and the mean value was recorded for further analysis. The ultrasound scan was made by the same investigator with good test consistency (ICC = 0.99).

### Maximum isometric elbow flexion torque

Maximum isometric elbow flexion torque ( $MVC_{EF}$ ) on the dominant side was recorded using a customized dynamometer (MMU, UK), which was calibrated using loads of 0.5–5 kg (with 0.5 kg increments) prior to each strength measurement session. Participants were tested in a seated position with the upper arm parallel to the trunk and the elbow flexed at 60° (0° representing full extension). Participants were asked to hold a force transducer (connected to the dynamometer) and contract their elbow flexors with full effort. Verbal encouragement was given during the test. Three trials were performed with 1 min rest between each trial (ICC = 0.95), with the highest  $MVC_{EF}$  used for analysis. Elbow force was recorded at 1000 Hz and analysed offline at a later date (Labview, National Instruments, Newbury, UK).  $MVC_{EF}$  was calculated by the formula:  $MVC_{EF} = \text{Elbow force} \times \text{Radius length} \times \cos(30^\circ)$  with force in N and length in metres.

### Maximum isometric knee extension torque

Maximum isometric knee extension torque ( $MVC_{KE}$ ) on the dominant side was recorded using the same system as that used in  $MVC_{EF}$  measurement. Participants were tested in a seated position with 60° knee flexion (0° representing full extension). The tested leg was fastened to a force transducer placed 5 cm above the lateral malleolus. Participants were instructed to extend the fastened leg, and verbal encouragement was given during the measurement. Three trials were performed with 1 min break between each trial (ICC = 0.96), with the highest  $MVC_{KE}$  used for analysis. Knee force was recorded at 1000 Hz and analysed offline at a later date (Labview, National Instruments, Newbury, UK).  $MVC_{KE}$  was calculated by the formula:  $MVC_{KE} = \text{Knee force} \times (\text{Tibia length} - 0.05) \times \cos(30^\circ)$  with force in N and length in metres.

## Statistics, model building, and model evaluation

### Statistics

SAS 9.4 (SAS Institute, Cary, NC, US) and Python (version 3.7.3) were used for data management and data analysis. Comparisons of muscular phenotypes and methylation scores between the sarcopenic and non-sarcopenic groups were made using independent *t*-tests. Fisher's exact test was used to compare the distribution of GPS between the two groups. To study combined genetic and epigenetic associations with skeletal muscle, three linear regression models (Models 1–3, Figure 1) were built with muscular phenotypes ( $THK_{BB}$ ,  $ACSA_{VL}$ ,  $MVC_{EF}$ , and  $MVC_{KE}$ ) as dependent variables and genetic and epigenetic scores as independent variables. Linear models (Models 4–6) with only a genetic or methylation score were also built to study the single genetic or methylation association with muscular phenotypes. All models were adjusted for age and BMI. Data are presented as mean and standard deviation.

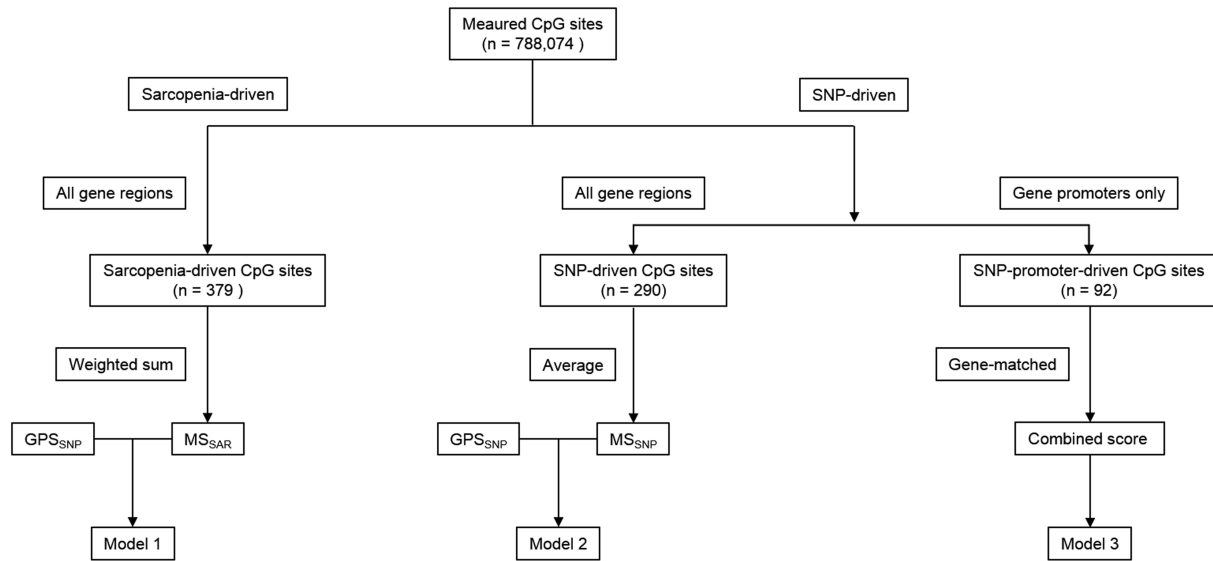


FIGURE 1 Workflow for model building (Model 1–3).

**Model building**

Model 1: muscular phenotypes ~ sarcopenia-driven methylation score (MS<sub>SAR</sub>) + muscle-driven genetic predisposition score (GPS<sub>SNP</sub>)

This model aimed to analyse the association between muscular phenotypes, muscle-related genetic architecture and sarcopenia-driven methylation levels using a muscle-driven genetic score and a sarcopenia-driven methylation score as independent variables. The least absolute shrinkage and selection operator (LASSO) logistic regression was used for sarcopenia-driven CpG sites selection. The LASSO method combines a linear regression with a L1 penalty on independent variable coefficients to improve prediction accuracy and reduce overfitting.<sup>44</sup> Through a shrinkage parameter tuning, the LASSO method aims to minimize residual sum of squares by setting some coefficients of independent variables to zeros.<sup>44</sup> Therefore, the LASSO method is a powerful tool of selecting strong independent variables from a large set of candidate variables when the amount of independent variables greatly outnumbers the amount of observations.<sup>44</sup> Cross validation is usually used to find an optimal shrinkage parameter.

In the current study, the sarcopenia status was used as the dependent variable (sarcopenia coded as 1 and non-sarcopenia coded as 0) and the methylation levels (β values) at measured CpG sites were used as independent variables. A six-fold cross validation (with the log loss score, the accuracy score and the F1 score as metrics) was used for shrinkage parameter tuning (Figure S2, Supplementary Table S2A). The sarcopenia-driven LASSO regression with an optimal shrinkage parameter selected CpGs (with non-zero coefficients) that were strongly associated with sarcopenia status. The MS<sub>SAR</sub> was calculated as a weighted sum of the selected CpG methylation levels (the weight for each CpG site was the

coefficient from the LASSO regression, Supplementary Table S2B, codes in Supplementary File 1). The ‘gene symbols’ of selected CpG sites were further analysed by gene ontology (GO) and KEGG analysis (databases until June 2019) using Partek Genomics Suite V.7.18 (Partek Inc., St. Louis, MO, US) (‘HumanMethylation850’ reference, ‘MethylationEPIC\_v-1-0\_B4’ annotation file, ‘Homo sapiens’ species and hg19 genome build) with a false discovery rate (FDR) control at 0.05.

A summed score of the seven muscle-related SNPs (Table S1) was calculated as GPS<sub>SNP</sub>. Each SNP score was represented by the number of muscle-favourable alleles. For example, the C allele is a muscle-favourable allele in the *ACTN3* rs1815739. Therefore, the SNP score of the *ACTN3* rs1815739 is 2 for a CC genotype, 1 for a CT genotype and 0 point for a TT homozygote.

Model 2: muscular phenotypes ~ SNP-driven methylation score (MS<sub>SNP</sub>) + GPS<sub>SNP</sub>

To evaluate the association between muscle-related genes and muscular phenotypes, this model only included genetic and methylation scores within genes where the seven muscle-related SNPs locate (Table S2C). Because each muscle-related gene contained different amounts of measured CpGs, the mean methylation level of each gene was firstly calculated and the MS<sub>SNP</sub> was later calculated as the mean of the mean methylation levels of the seven muscle-related genes. Using *n<sup>i</sup>* to represent the number of measured CpGs in the *i*th gene, *M<sub>j</sub><sup>i</sup>* to represent the methylation level of the *j*th measured CpG in the *i*th gene, then the calculation of the MS<sub>SNP</sub> can be represented as:

$$MS_{SNP} = \left( \sum_{i=1}^7 \left( \left( \sum_{j=1}^{n^i} M_j^i \right) / n^i \right) \right) / 7$$

Model 3: muscular phenotypes ~ seven gene-wise combined genetic and methylation scores

This model examined each of the seven selected muscle-related gene and studied its association with muscular phenotypes by building a gene-wise combined genetic and methylation profile score. In this model, a methylation score was calculated as the mean methylation level of promoters in each gene because, compared to other gene regions, increased methylation in gene promoters has been more strongly associated with a repression of gene expression.<sup>21</sup> The gene-wise combined score was later calculated as the ratio of a SNP score to the mean methylation level in promoters of the corresponding gene (*Table S2D*) so that a participant with a higher SNP score and a lower methylation score would have a higher gene-wise combined score. For instance, there were five measured CpG sites located in the promoters of *MSTN*. Given that one participant has a *MSTN* SNP (rs1805086) score of 2 and a mean methylation level of 0.32 at the five CpG sites located in *MSTN* promoters, the *MSTN*-wise combined score will be 6.26; if another participant has a *MSTN* SNP score of 1 and a mean promoter methylation level of 0.4, then the *MSTN*-wise combined score will be 2.5. Similar calculations were carried out in the other six genes and therefore, there were seven gene-wise combined scores (representing each of the seven muscle-related genes) as independent variables in Model 3.

Model 4: muscular phenotypes ~  $MS_{SAR}$

This model only studied the association between the sarcopenia-driven methylation and muscular phenotypes.

Model 5: muscular phenotypes ~  $MS_{SNP}$

This model only studied the association between the methylation of muscle-related genes and muscular phenotypes.

Model 6: muscular phenotypes ~  $GPS_{SNP}$

This model only studied the association between the muscle-related genetic architecture and muscular phenotypes.

#### Model interpretation and evaluation

Adjusted coefficient of determination ( $R^2$ ) was used to interpret the explained variance in muscular phenotypes by each linear model. Because a model with more independent variables usually has a higher  $R^2$ , the adjusted  $R^2$  is introduced as a modification of the  $R^2$  controlled for the number of independent variables in the corresponding model. In this study, a partial  $R^2$  was also used to illustrate the phenotype variance that an independent variable accounted for in a linear model. The Akaike information criterion (AIC) was used to evaluate

the quality of each model with the same muscular phenotype as the dependent variable. The AIC assesses the relative amount of information lost by a given model;<sup>45</sup> therefore, the model with the smallest AIC will be the best model (among all candidate models). Empirically, if another model has an AIC value that is less than two units from the smallest AIC, then that model also has considerable ability to explain variability in the corresponding dependent variable. In that case, more data are needed for model evaluation or a combined model should be created for a better prediction.<sup>46</sup>

## Results

### Characteristics of participants

Descriptive characteristics of participants are presented in *Table 1*. Participants in the sarcopenic group had lower body mass ( $P = 0.003$ ) and BMI ( $P = 0.005$ ) than the non-sarcopenic group. Values of muscular phenotypes in the sarcopenic group were lower ( $P < 0.001$ ) than in the non-sarcopenic group, except for  $THK_{BB}$  ( $P = 0.283$ ).

Comparisons of methylation scores are presented in *Table 2*. The sarcopenic group had a higher  $MS_{SAR}$  than the non-sarcopenic group ( $P < 0.001$ , *Figure 2A*), and the combined genetic and methylation score in *VDR* was lower in the sarcopenic group ( $P = 0.02$ ). The mode and median values of  $GPS_{SNP}$  were both 9 in the non-sarcopenic group, and the mode and median values of  $GPS_{SNP}$  in the sarcopenic group were 7 and 8, respectively. Fisher's exact test for the distribution of  $GPS_{SNP}$  between the sarcopenic and non-sarcopenic group showed no difference ( $P = 0.67$ , *Figure 2C*).

### CpG sites selected from the sarcopenia-driven LASSO logistic regression

Three hundred seventy-nine CpG sites were selected from the sarcopenia-driven LASSO logistic regression, indicating a possible association between these CpGs and sarcopenia. These selected CpGs located in 190 genes, with the *PIWIL1* gene contributing most ( $n = 4$ ) CpGs (*Table S3A*). GO analysis on the identified genes showed that 29 GO terms were enriched after FDR control ( $q$  value  $< 0.05$ , *Table S3B*). Many of these GO terms were associated with protein binding (e.g. antigen binding and cell adhesion), MHC protein complex, signal transduction (e.g. receptor binding and transport vesicle membrane), and synapse structure (e.g. synapse assembly and synapse organization). The most enriched GO term was the 'peptide antigen binding' term ( $q$  value = 0.002), which included four hypermethylated (higher methylation in the sarcopenic group than non-sarcopenic group) CpGs and three hypomethylated (lower methylation in the sarcopenic group) CpGs (*Table S3C*). KEGG analysis showed 46 pathways that were enriched ( $q$  value  $< 0.05$ , *Table S3D*). Many pathways

**Table 1** Characteristics of participants (*n* = 48)

Participants	Age (year)	Body mass (kg)	Height (m)	BMI (kg/m <sup>2</sup> )	HGS (kg)	SMI (kg/m <sup>2</sup> )	THK <sub>BB</sub> (cm)	ACSA <sub>VL</sub> (cm <sup>2</sup> )	MVC <sub>EF</sub> (N·m)	MVC <sub>KE</sub> (N·m)
Total ( <i>n</i> = 48)	71 ± 4	66.6 ± 12.3	1.59 ± 0.06	26.2 ± 4.5	29.6 ± 7.1**	6.72 ± 0.93**	1.82 ± 0.35	16.4 ± 3.9	25.0 ± 5.8**	58.8 ± 19.9*
Sarcopenic ( <i>n</i> = 24)	73 ± 4	61.5 ± 9.4**	1.56 ± 0.11	24.4 ± 3.4**	23.2 ± 2.5**	6.00 ± 0.47**	1.76 ± 0.38	14.3 ± 3.0**	21.2 ± 4.8**	44.9 ± 10.2*
Non-sarcopenic ( <i>n</i> = 24)	70 ± 3	71.7 ± 12.8	1.60 ± 0.05	28.0 ± 4.9	36.0 ± 3.7	7.45 ± 0.67	1.88 ± 0.33	18.2 ± 3.7	28.7 ± 4.1	71.0 ± 18.3

\*Lower than non-sarcopenic group (*P* < 0.05).

\*\*Lower than non-sarcopenic group (*P* < 0.01).

**Table 2** Description of genetic and methylation profile scores in different groups.

Participants	MS <sub>SAR</sub>	MS <sub>SNP</sub>	Gene-wise combined genetic and methylation scores						
			ACTN3_combined	ACE_combined	CNTF_combined	FTO_combined	HIF1A_combined	MSTN_combined	VDR_combined
Total ( <i>n</i> = 48)	0.02 ± 5.26 <sup>#</sup>	0.64 ± 0.01	7.27 ± 5.78	2.73 ± 1.73	2.14 ± 0.46	3.73 ± 2.88	1.02 ± 2.15	2.16 ± 0.02	5.43 ± 2.93
Sarcopenic ( <i>n</i> = 24)	5.21 ± 0.53 <sup>#</sup>	0.64 ± 0.01	7.53 ± 6.02	2.68 ± 1.59	2.12 ± 0.49	3.90 ± 3.06	0.91 ± 2.08	2.16 ± 0.02	4.46 ± 2.93*
Non-sarcopenic ( <i>n</i> = 24)	-5.17 ± 0.37	0.64 ± 0.01	7.01 ± 5.65	2.78 ± 1.88	2.16 ± 0.44	3.55 ± 2.73	1.13 ± 2.26	2.16 ± 0.02	6.39 ± 2.65

\*Lower than non-sarcopenic group (*P* < 0.05).

<sup>#</sup>Greater than non-sarcopenic group (*P* < 0.01).



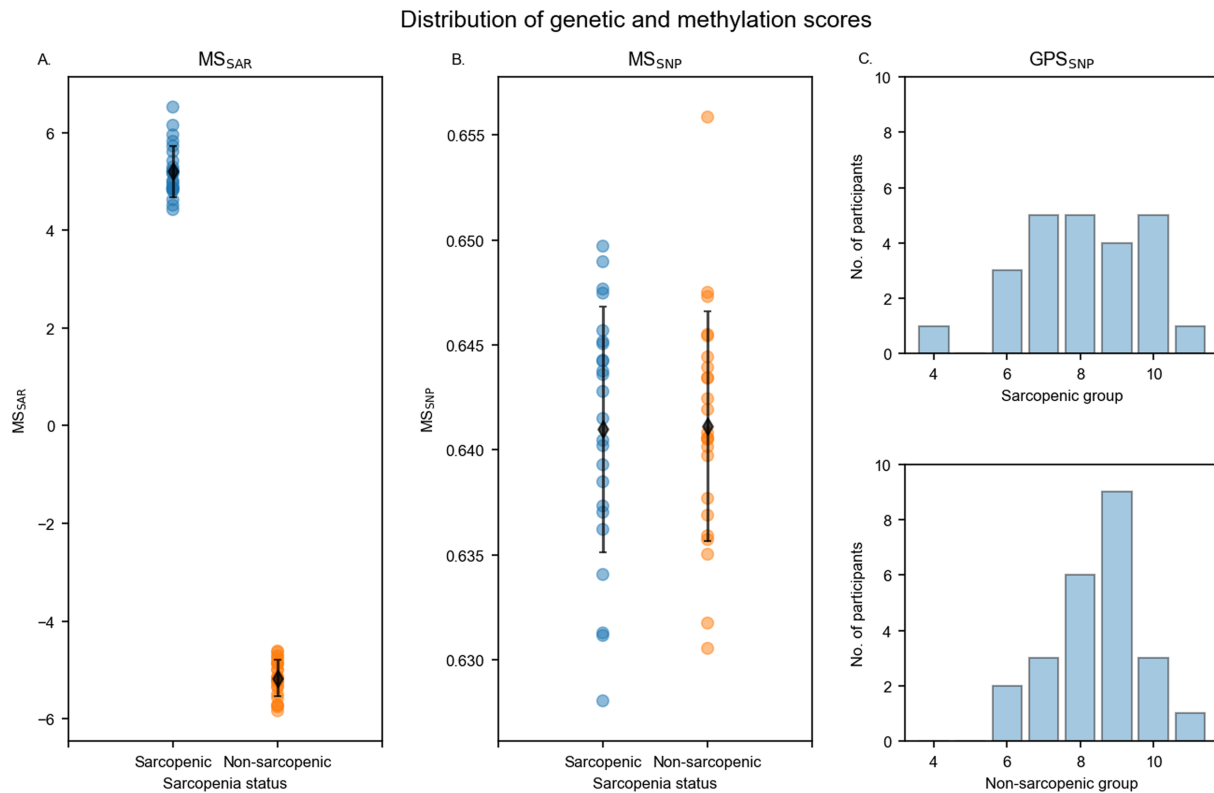


**FIGURE 2** Distribution of genetic and methylation profile scores. (A)  $MS_{SAR}$  based on CpGs selected by sarcopenia-driven LASSO regression is higher in the sarcopenic than the non-sarcopenic group ( $p < 0.01$ ). Black diamond markers represent the mean  $MS_{SAR}$  in each group. (B)  $MS_{SNP}$  is not different between the sarcopenic and non-sarcopenic groups ( $p = 0.96$ ). (C) Fisher's exact test for the distribution of  $GPS_{SNP}$  showed no difference between the sarcopenic and non-sarcopenic group ( $p = 0.67$ ).

were related to immune system function (e.g. allograft rejection and T helper cells differentiation) and diseases (e.g. autoimmune thyroid disease and viral myocarditis), and chronic disorders (e.g. type I diabetes mellitus and rheumatoid arthritis). The most enriched pathway was the 'Asthma' pathway with three hypermethylated CpGs and four hypomethylated CpGs (Table S3E).

### Muscular phenotypes with genetic and methylation scores

Main results of linear regression models with both genetic and methylation scores are presented in Table 3 (complete results in Table S4). In Model 1, the  $MS_{SAR}$  was negatively related to  $MVC_{EF}$  and  $MVC_{KE}$  ( $P < 0.01$ ) and explained 33.2% and 39.4% of the variance, respectively. With one unit increase in the  $MS_{SAR}$ ,  $MVC_{EF}$  and  $MVC_{KE}$  decreased by 0.67 and 2.63 N·m, respectively. The  $GPS_{SNP}$  was not significantly associated with any muscular phenotypes. In Model 2, neither the  $MS_{SNP}$  nor the  $GPS_{SNP}$  was significantly correlated to muscular phenotypes. In Model 3, only the combined genetic and methylation score in the *CNTF* was positively related to  $MVC_{KE}$  ( $P = 0.03$ ) and explained 12.2% of the

$MVC_{KE}$  variance. A one-score addition in the *CNTF* combined score was associated with 15.7 N·m increase in  $MVC_{KE}$ .

Results of linear models with only a genetic/methylation score are presented in Table 4 (complete results in Table S4). The  $MS_{SAR}$  alone (Model 4) was negatively associated with  $ACSA_{VL}$ ,  $MVC_{EF}$ , and  $MVC_{KE}$ , and explained 10.1%, 35.5%, and 40.1% of the variance, respectively. The  $MS_{SNP}$  and  $GPS_{SNP}$  were not associated with any muscular phenotypes. Specifically, the  $MS_{SNP}$  explained less than 8% of the variance in muscle size and less than 1% of the variance in muscle strength. The  $GPS_{SNP}$  accounted for less than 5% of the variance in all muscular phenotypes.

Explained variance of muscular phenotypes by the six models are presented in Table 5. Model 1 with both the  $MS_{SAR}$  and  $GPS_{SNP}$  explained less phenotype variance than Model 4, which included only an  $MS_{SAR}$ , and more variance in muscle strength than Model 6, which included only a  $GPS_{SNP}$ . Model 2 with the  $MS_{SNP}$  and  $GPS_{SNP}$  explained less variance in muscle size than Model 5. When compared with Model 6, Model 2 explained more variance in muscle size but less variance in muscle strength. Models with an  $MS_{SAR}$  (Models 1 and 4) explained more variance in muscle strength ( $MVC_{EF}$  and  $MVC_{KE}$ ) than models without  $MS_{SAR}$ . When comparing models with genetic and methylation profile scores within the preselected

**Table 3** Main results of linear models (Models 1–3) with combined genetic and methylation scores

	Model 1				Model 2				Model 3		
	MS <sub>SAR</sub>	GPS <sub>SNP</sub>	Age	BMI	MS <sub>SNP</sub>	GPS <sub>SNP</sub>	Age	BMI	CNTF_combined	Age	BMI
THK <sub>BB</sub>											
Coef	<0.01	-0.01	0.03	0.04	-16.47	-0.02	0.04	0.04	0.09	0.03	0.04
Partial R <sup>2</sup>	0.002	0.003	0.145	0.201	0.080	0.007	0.198	0.270	0.017	0.142	0.258
P	0.76	0.74	0.01	<0.01	0.07	0.60	<0.01	<0.01	0.44	0.02	<0.01
ACSA <sub>VL</sub>											
Coef	-0.16	0.16	-0.02	0.57	-97.93	0.26	-0.02	0.64	1.33	-0.04	0.73
Partial R <sup>2</sup>	0.080	0.008	0.001	0.499	0.041	0.023	0.001	0.591	0.052	0.004	0.614
P	0.07	0.56	0.89	<0.01	0.20	0.34	0.84	<0.01	0.18	0.72	<0.01
MVC <sub>EF</sub>											
Coef	-0.67	0.29	-0.05	0.08	-23.51	0.78	-0.27	0.37	2.02	-0.24	0.42
Partial R <sup>2</sup>	0.332	0.009	0.001	0.006	0.001	0.042	0.033	0.086	0.023	0.026	0.094
P	<0.01	0.55	0.81	0.62	0.88	0.18	0.23	0.05	0.36	0.33	0.06
MVC <sub>KE</sub>											
Coef	-2.63	-0.37	-0.58	-0.53	193.22	1.56	-1.30	0.72	15.68	-0.99	1.70
Partial R <sup>2</sup>	0.394	0.001	0.019	0.021	0.003	0.014	0.053	0.028	0.122	0.042	0.142
P	<0.01	0.82	0.38	0.36	0.74	0.45	0.14	0.29	0.03	0.22	0.02

seven muscle-related genes, Model 3 explained less variance than Model 2 in all muscular phenotypes except for MVC<sub>KE</sub>. Notably, the explained variance in muscle size (THK<sub>BB</sub> and ACSA<sub>VL</sub>) was similar across all models. This was possibly because BMI was closely related to muscle size and explained a considerable percentage (20.1% to 61.4%) of the variance (Tables 3 and 4).

In the aspect of model evaluation, Model 5, which included only an MS<sub>SNP</sub>, explained the most variance in THK<sub>BB</sub> (with the highest adjusted R<sup>2</sup> value) and outperformed other models in the prediction of THK<sub>BB</sub> (with the lowest AIC value). Model 4, which includes only an MS<sub>SAR</sub>, explained the most variance in ACSA<sub>VL</sub>, MVC<sub>EF</sub>, and MVC<sub>KE</sub> (with the highest adjusted R<sup>2</sup> values), and performed better than other models in the prediction of those muscular phenotypes (ACSA<sub>VL</sub>,

MVC<sub>EF</sub>, and MVC<sub>KE</sub>) (with the lowest AIC values). Notably, the AIC differences were smaller than two between Models 2 and 5 (in THK<sub>BB</sub>), and Models 1 and 4 (in ACSA<sub>VL</sub>, MVC<sub>EF</sub>, and MVC<sub>KE</sub>), indicating that more data might be needed before deciding if GPS<sub>SNP</sub> should be included into a model.

*Correlation and regression analysis on actual and predicted muscle size values inferred by Model 4*

As Model 4 is the most powerful model in predicting muscular phenotypes than the rest models in Table 5, correlation analysis was made between actual and predicted muscle size inferred by Model 4. Moderate correlations ranging between 0.55 and 0.79 were found (Figure 3, Supplementary Table 4F).

**Table 4** Main results of linear models (Models 4–6) with only genetic or methylation scores

	Model 4			Model 5			Model 6		
	MS <sub>SAR</sub>	Age	BMI	MS <sub>SNP</sub>	Age	BMI	GPS <sub>SNP</sub>	Age	BMI
THK <sub>BB</sub>									
Coef	<0.01	0.03	0.04	-15.80	0.04	0.04	-0.01	0.03	0.04
Partial R <sup>2</sup>	0.001	0.147	0.211	0.075	0.194	0.272	0.002	0.147	0.248
P	0.82	0.01	<0.01	0.07	<0.01	<0.01	0.80	0.01	<0.01
ACSA <sub>VL</sub>									
Coef	-0.17	<0.01	0.57	-107.42	<0.01	0.64	0.31	-0.07	0.64
Partial R <sup>2</sup>	0.101	<0.001	0.496	0.048	<0.001	0.583	0.031	0.009	0.579
P	0.04	1.00	<0.01	0.16	0.98	<0.01	0.26	0.54	<0.01
MVC <sub>EF</sub>									
Coef	-0.69	-0.02	0.06	-51.35	-0.22	0.34	0.79	-0.28	0.37
Partial R <sup>2</sup>	0.355	<0.001	0.004	0.003	0.022	0.074	0.044	0.036	0.087
P	<0.01	0.90	0.69	0.73	0.33	0.07	0.17	0.21	0.05
MVC <sub>KE</sub>									
Coef	-2.60	-0.61	-0.51	115.81	-1.17	0.68	1.45	-1.21	0.72
Partial R <sup>2</sup>	0.401	0.022	0.020	0.001	0.044	0.026	0.013	0.051	0.029
P	<0.01	0.34	0.37	0.84	0.18	0.31	0.47	0.15	0.28

**Table 5** Adjusted  $R^2$  and AIC of linear models

	Model 1	Model 2	Model 3	Model 4	Model 5	Model 6
<b>THK<sub>BB</sub></b>						
Adj $R^2$	0.240	0.299	0.255	0.256	0.311	0.256
AIC	-103.5	-107.2	-100.4	-105.4	-108.9	-105.4
<b>ACSA<sub>VL</sub></b>						
Adj $R^2$	0.585	0.568	0.561	0.592	0.568	0.560
AIC	86.4	88.3	92.9	84.8	87.3	88.1
<b>MVC<sub>EF</sub></b>						
Adj $R^2$	0.371	0.060	-0.013	0.380	0.042	0.081
AIC	148.4	167.3	174.8	146.8	167.3	165.3
<b>MVC<sub>KE</sub></b>						
Adj $R^2$	0.392	<.001	0.112	0.406	0.010	0.021
AIC	251.4	273.8	272.5	249.5	272.5	272.0

## Discussion

The current study explored the association between muscular phenotypes, genetic architecture, and DNA methylation via linear regression models in sarcopenic and non-sarcopenic elderly women. Genetic architecture was represented as a GPS that was calculated from seven muscle-related SNPs. The DNA methylation was represented as either a sarcopenia-driven methylation score, which was calculated as a weighted sum of the methylation levels of 379 sarcopenia-driven CpG sites, or a gene-wise methylation score, which was calculated as an average of the methylation levels within muscle-related genes. Based on the six linear models used in this study, the sarcopenia-driven methylation score was negatively related to ACSA<sub>VL</sub>, MVC<sub>EF</sub>, and MVC<sub>KE</sub>, and explained more variance in these muscular phenotypes than the GPS, the gene-wise methylation score and the models with combined genetic and methylation scores. The adjusted  $R^2$  and AIC showed that models with only a methyl-

ation score had the best performance in explaining inter-individual variance in muscular phenotypes while more data are needed to determine the inclusion of GPS into the models. Moreover, the model with gene-wise combined genetic and methylation scores demonstrated that the genotype and methylation level in *CNTF* was closely related to knee extensor strength, indicating a close association between *CNTF* and knee strength.

### Sarcopenia-driven CpG sites

DNA methylation changes have been examined in studies of ageing and resistance training, but no study has reported the DNA methylation association with sarcopenia. Using the sarcopenia-driven LASSO logistic regression, our study identified 379 CpG sites that were possibly related to sarcopenia. Zykovich *et al.*<sup>24</sup> identified 5963 CpG sites that were related to ageing based on skeletal muscle tissue. Bell *et al.*<sup>47</sup> found 490 ageing-associated CpGs from blood samples. However, none of those ageing-related CpGs were found among the sarcopenia-driven CpGs identified in our study. Seaborne *et al.* studied DNA methylation changes in skeletal muscle during resistance training and identified 2445 CpG sites that were differentially methylated after a 7-week loading stimuli and 1883 CpGs that were association with an unloading phase. We shared one CpG site in each of the loading and unloading phase, with both CpGs located in the intergenic region (Table S5A). We further compared our CpGs with those identified by Turner *et al.*,<sup>34</sup> who analysed transcriptome and methylome associations after acute/chronic resistance training, but no common CpG was found. Notably, Turner *et al.* reported three genes (*ETF1*, *ETV1*, and *SH3KBP1*) that were up-regulated after acute/chronic resistance training<sup>34</sup> while some hypermethylated sarcopenia-driven

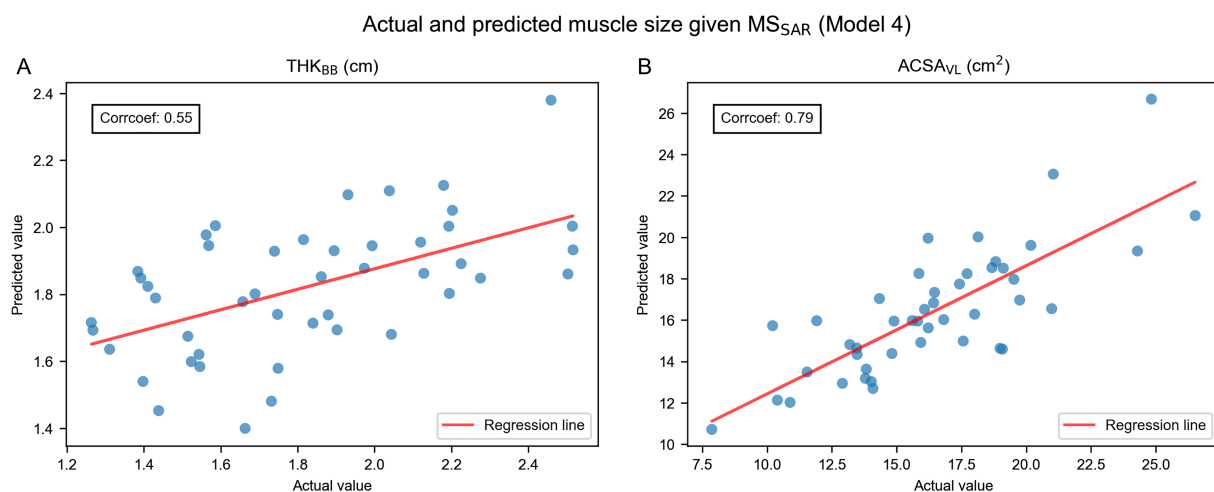


**FIGURE 3** Plots of actual and predicted muscle size inferred by Model 4. (A) Actual and predicted THK<sub>BB</sub> values are moderately correlated ( $r = 0.55$ ). (B) Actual and predicted ACSA<sub>VL</sub> values are moderately correlated ( $r = 0.79$ ).

CpGs identified in our study were found to locate in promoter regions of those three genes (*Tables S5B,C, S3*).

The gene *ETF1* is a member of the human transcriptional enhancer family. Recent research on human liver HepG2 cell line showed that the *ETF1* gene was involved in the regulation of transcript stability.<sup>48</sup> The gene *ETV1* is involved in multiple cellular activities that are related to physical performance. *ETV1* knockout mice demonstrated abnormal cardiac conduction<sup>49</sup> and neuromuscular impairment.<sup>50</sup> The gene *SH3KBP1* belongs to a gene group of putative motility modifiers, and the knocking down of *SH3KBP1* leads to reduced cell migration in scratch wound assays.<sup>51</sup> Because it has been established that hypermethylated gene promoters are associated with repressed gene expression,<sup>52</sup> the identification of hypermethylated CpGs in promoters of these three genes (*ETF1*, *ETV1*, and *SH3KBP1*) in our study indicates possible down-regulated cellular activity in association with sarcopenia. Yet further transcriptome analysis on corresponding genes are still needed to confirm the down-regulation in gene expression.

### Evaluation of linear models

In our study, the sarcopenia-driven methylation score ( $MS_{SAR}$ ) was closely related to muscle strength and explained 33.2% to 40.1% of inter-individual variance in all models (Models 1 and 4). This indicates a possible application of the  $MS_{SAR}$  to the estimation of skeletal muscle strength in older women. Meanwhile, we should be aware that the participants in this study belong to two groups (i.e. sarcopenic and non-sarcopenic groups) which have significant difference in muscle strength (*Table 1*) and  $MS_{SAR}$  (*Table 2*). Therefore, when applying the  $MS_{SAR}$  to a population with less variability in muscle strength (e.g. a group with only physically fit older people or a group with only sarcopenic participants), the corresponding muscular variance explained by the  $MS_{SAR}$  might decrease to some extent. In fact, the  $MS_{SAR}$  was found to explain less than 8% of the muscular variance within the sarcopenic or non-sarcopenic group when analysed separately (*Table S4E*). Clearly, future studies on larger cohorts are still needed to evaluate the feasibility of applying the  $MS_{SAR}$  for muscle strength evaluation.

Additionally, we found that genetic profile scores based on seven selected genes ( $GPS_{SNP}$ ) explained up to 4.4% of the variance in muscle size and strength, methylation levels in the seven selected genes ( $MS_{SNP}$ ) explained up to 8% in the studied phenotypes, while the  $MS_{SAR}$  explained 10.1–40.1% of the individual differences in muscle size and strength in our sample of older women. These results showed that genetic and methylation profiles on several representative genes only explained limited muscular variability. Moreover, by comparing the AIC, the model with only an  $MS_{SAR}$  showed the best performance in explaining the variance in muscle

size and strength. This, again, indicated that using the data from a small set of representative genes might not well explain muscular variability. Notably, previous studies have demonstrated that even based on a larger candidate pool of more than 100 genetic variants, the data-driven GPS only explained up to 7% of the variance in muscle mass and strength.<sup>16,53</sup> Therefore, it is possible that the genetic architecture only accounts for a small portion of muscular variability during ageing—or we have not yet used the optimal methodology to include all contributing genetic factors, while a larger proportion of the variance is taken up by DNA methylation. Because DNA methylation is representing the sum of short-term and long-term environmental factors, the finding that methylation levels explains a larger proportion of the variance in muscle morphology and strength than genetic profiles might indicate that environmental elements account for more variance than genetic factors in skeletal muscle during ageing, which is in line with the findings of previous heritability studies.<sup>6,54,55</sup>

Notably, the model with gene-wise combined genetic and methylation score (Model 3) showed that the genotype and methylation level in *CNTF* was closely related to knee extensor strength. The *CNTF* gene encodes ciliary neurotrophic factor, a polypeptide that promotes neuronal cell differentiation and neurite outgrowth, and exerts a neuroprotective effect by preventing motor neuron degeneration.<sup>56</sup> Indeed, *CNTF* G allele carriers have shown higher knee strength than A allele homozygotes at both slow and fast contraction speed across a large age span (20–90 years).<sup>57</sup> Our finding provides supportive evidence for the association between *CNTF* and knee strength.

### Limitations

We acknowledge that, despite presenting significant associations, our study has a limited sample size. Because of the limited sample size, we could only use adjusted  $R^2$  and AIC for model evaluation. Therefore, our results still need to be examined in different cohorts with large sample sizes. Moreover, DNA methylation is only one mechanism of epigenetic regulation. Future models including other epigenetic mechanisms (e.g. histone methylation and acetylation), genome conformation, and transcriptome analysis might make the model more reliable. Additionally, the current study still remains descriptive and only reports the CpG sites that might be associated with sarcopenia based on the results of statistical analysis. Further transcriptome analysis on the genes, where these sarcopenia-driven CpG sites (identified in the current study) located, should give more insight into the DNA methylation association with gene expression in respect of skeletal muscle condition among older women.

Another limitation is that the methylation data used in this study were based on blood samples. It is well known that

DNA methylation is tissue-specific,<sup>58</sup> so the methylation data obtained from blood might not fully represent the methylation status in other tissues. Although venous blood is more easily obtained, methylation status could be more informative if DNA was derived from skeletal muscle tissue. Meanwhile, the Illumina MethylationEPIC BeadChip used for methylation analysis in our study only covers 850 K CpG sites, which is a small proportion of the 28 million CpG sites in the human genome, and is not always informative because many CpG sites are omitted.<sup>41</sup> Therefore, a methylome-wide association study should be more powerful in identifying sarcopenia-driven or muscle-related CpG sites for model building.

## Conclusions

Our study combined genotypes and DNA methylation levels to evaluate their associations with muscle size and strength in older women. We found that a sarcopenia-driven methylation score explained more inter-individual variance in muscle strength and thigh muscle size than a genetic score or models with both genetic and methylation scores. Our results suggest a possible application of a sarcopenia-driven methylation score to identify older adults who are at risk of muscle weakness conditions (e.g. sarcopenia and frailty) using routine blood samples, while the combination with a genetic score still needs to be further studied.

## Acknowledgements

This study is supported by the Research Foundation—Flanders (FWO) [grant G.0898.15] and a PhD grant to Lingxiao He and Praval Khanal by the Erasmus Mundus ‘Move-AGE’ joint doctorate program.

## Online supplementary material

Additional supporting information may be found online in the Supporting Information section at the end of the article.

Data S1. Supporting information

Table S1 SNPs selected in our study

## References

1. McLeod M, Breen L, Hamilton DL, Philp A. Live strong and prosper: the importance of skeletal muscle strength for healthy ageing. *Biogerontology* 2016;**17**:1–14.
2. Visser M, Goodpaster BH, Kritchevsky SB, Newman AB, Nevitt M, Rubin SM, et al.

Table S2. Supporting information

Table S3. Supporting information

Table S4. Supporting information

Table S5. Supporting information

Figure S1. Ultrasound images of the upper arm and the thigh. a. Ultrasound image of the upper arm (Sagittal); b. Ultrasound image of the thigh (cross-sectional).

Figure S2. Shrinkage parameter tuning for sarcopenia-driven LASSO logistic regression. The red line represents the mean value of corresponding metric in a six-fold cross validation. The light blue area between the two blue dash lines marks out the range one standard deviation away from the mean value. The orange line demonstrates the optimal shrinkage parameter (C) with the best metric value. a. Changes of the log loss score with the shrinkage parameter. The log loss score reaches an optimal value of 0.69 when C is 65.13; b. Changes of the accuracy score with the shrinkage parameter. The accuracy score reaches an optimal value of 0.6 when C is 65.13; c. Changes of the F1 score with the shrinkage parameter. The F1 score reaches an optimal value of 0.63 when C is 65.13.

Figure S3. CpG sites (cg24840200, cg17629006, cg21402738 and cg18811601 shared with Turners study) located in gene promoters. The location information is obtained using UCSC Genome Browser on Human Feb. 2009 (GRCh37/hg19) Assembly. Gene annotation is provided by RefSeq Transcripts 92. Each plot consists of three layers. The top layer shows the gene location on the chromosome. The middle layer presents the gene regions and the promoter region where the CpG site is located. The bottom layer demonstrates the beta value of each participant (marked by the sarcopenic and non-sarcopenic groups).

## Conflict of interest

The authors declare no conflicts of interest. The authors certify that they comply with the ethical guidelines for publishing in the *Journal of Cachexia, Sarcopenia and Muscle*: update 2017.<sup>59</sup>

- Muscle mass, muscle strength, and muscle fat infiltration as predictors of incident mobility limitations in well-functioning older persons. *Journals Gerontol - Ser A Biol Sci Med Sci* 2005;**60**:324–333.
3. Landi F, Liperoti R, Russo A, Giovannini S, Tosato M, Capoluongo E, et al. Sarcopenia as a risk factor for falls in elderly individuals: results from the iSIRENTE study. *Clin Nutr* 2012;**31**:652–658.
  4. Balogun S, Winzenberg T, Wills K, Scott D, Jones G, Callisaya ML, et al. Prospective associations of low muscle mass and strength with health-related quality of life over 10-year in community-dwelling older adults. *Exp Gerontol* 2019;**118**:65–71.
  5. Arden NK, Spector TD. Genetic influences on muscle strength, lean body mass, and bone mineral density: a twin study. *J Bone Miner Res* 1997;**12**:2076–2081.
  6. Carmelli D, Reed T. Stability and change in genetic and environmental influences on hand-grip strength in older male twins. *J Appl Physiol* 2000;**89**:1879–1883.
  7. Puthuchery Z, Skipworth JRA, Rawal J, Loosemore M, Van Someren K, Montgomery HE. The ACE gene and human performance: 12 years on. *Sport Med* 2011;**41**:433–448.
  8. Charbonneau DE, Hanson ED, Ludlow AT, Delmonico MJ, Hurley BF, Roth SM. ACE genotype and the muscle hypertrophic and strength responses to strength training. *Med Sci Sports Exerc* 2008;**40**:677–683.
  9. Erskine RM, Williams AG, Jones DA, Stewart CE, Degens H. The individual and combined influence of ACE and ACTN3 genotypes on muscle phenotypes before and after strength training. *Scand J Med Sci Sports* 2014;**24**:642–648.
  10. Vincent B, De Bock K, Ramaekers M, Van den Eede E, Van Leemputte M, Hespel P, et al. ACTN3 (R577X) genotype is associated with fiber type distribution. *Physiol Genomics* 2007;**32**:58–63.
  11. Heffernan SM, Stebbings GK, Kilduff LP, Erskine RM, Day SH, Morse CI, et al. Fat mass and obesity associated (FTO) gene influences skeletal muscle phenotypes in non-resistance trained males and elite rugby playing position. *BMC Genet* 2017;**18**:1–9.
  12. Williams AG, Folland JP. Similarity of polygenic profiles limits the potential for elite human physical performance. *J Physiol* 2008;**586**:113–121.
  13. Ruiz JR, Gómez-Gallego F, Santiago C, González-Freire M, Verde Z, Foster C, et al. Is there an optimum endurance polygenic profile? *J Physiol* 2009;**587**:1527–1534.
  14. Santiago C, Ruiz JR, Muniesa CA, González-Freire M, Gómez-Gallego F, Lucia A. Does the polygenic profile determine the potential for becoming a world-class athlete? Insights from the sport of rowing. *Scand J Med Sci Sport* 2010;**20**:e188–e194.
  15. Thomaes T, Thomis M, Onkelinx S, Goetschalckx K, Fagard R, Lambrechts D, et al. Genetic predisposition scores associate with muscular strength, size, and trainability. *Med Sci Sports Exerc* 2013;**45**:1451–1459.
  16. He L, Van Roie E, Bogaerts A, Morse CI, Delecluse C, Verschueren S, et al. Genetic predisposition score predicts the increases of knee strength and muscle mass after one-year exercise in healthy elderly. *Exp Gerontol* 2018;**111**:17–26.
  17. Jaenisch R, Bird A. Epigenetic regulation of gene expression: how the genome integrates intrinsic and environmental signals. *Nat Genet* 2003;**33**:245–254.
  18. Tammen SA, Friso S, Choi SW. Epigenetics: the link between nature and nurture. *Mol Aspects Med* 2013;**34**:753–764.
  19. Ehrlich M, Gama-Sosa MA, Huang LH, Midgett RM, Kuo KC, McCune RA, et al. Amount and distribution of 5-methylcytosine in human DNA from different types of tissues of cells. *Nucleic Acids Res* 1982;**10**:2709–2721.
  20. Martin EM, Fry RC. Environmental influences on the epigenome: exposure-associated DNA methylation in human populations. *Annu Rev Public Health* 2018;**39**:309–333.
  21. Deaton AM, Bird A. CpG islands and the regulation of transcription. *Genes Dev* 2011;**25**:1010–1022.
  22. Jeziorska DM, Murray RJS, De Gobbi M, Gaentzsch R, Garrick D, Ayyub H, et al. DNA methylation of intragenic CpG islands depends on their transcriptional activity during differentiation and disease. *Proc Natl Acad Sci* 2017;**114**:E7526–E7535.
  23. Mikeska T, Craig JM. DNA methylation biomarkers: cancer and beyond. *Genes (Basel)* 2014;**5**:821–864.
  24. Zykovich A, Hubbard A, Flynn JM, Tarnopolsky M, Fraga MF, Kerkisick C, et al. Genome-wide DNA methylation changes with age in disease-free human skeletal muscle. *Aging Cell* 2014;**13**:360–366.
  25. Hamilton OKL, Zhang Q, McRae AF, Walker RM, Morris SW, Redmond P, et al. An epigenetic score for BMI based on DNA methylation correlates with poor physical health and major disease in the Lothian Birth Cohort. *Int J Obes (Lond)* 2019;**43**:1795–1802.
  26. Ahmad AS, Vasiljević N, Carter P, Berney DM, Møller H, Foster CS, et al. A novel DNA methylation score accurately predicts death from prostate cancer in men with low to intermediate clinical risk factors. *Oncotarget* 2016;**7**.
  27. Zhao S, Leonardson A, Geybels MS, McDaniel AS, Yu M, Kolb S, et al. A five-CpG DNA methylation score to predict metastatic-lethal outcomes in men treated with radical prostatectomy for localized prostate cancer. *Prostate* 2018;**78**:1084–1091.
  28. Wei JH, Haddad A, Wu KJ, Zhao HW, Kapur P, Zhang ZL, et al. A CpG-methylation-based assay to predict survival in clear cell renal cell carcinoma. *Nat Commun* 2015;**6**:1–11.
  29. Reese SE, Zhao S, Wu MC, Joubert BR, Parr CL, Håberg SE, et al. DNA methylation score as a biomarker in newborns for sustained maternal smoking during pregnancy. *Environ Health Perspect* 2017;**125**:760–766.
  30. Bharathy N, Ling BMT, Taneja R. Epigenetic regulation of skeletal muscle development and differentiation. In *Epigenetics: Development and Disease*; 2013. p 139–150.
  31. Sharples AP, Polydorou I, Hughes DC, Owens DJ, Hughes TM, Stewart CE. Skeletal muscle cells possess a ‘memory’ of acute early life TNF- $\alpha$  exposure: role of epigenetic adaptation. *Biogerontology* 2016;**17**:603–617.
  32. Seaborne RA, Strauss J, Cocks M, Shepherd S, O’Brien TD, van Someren KA, et al. Human skeletal muscle possesses an epigenetic memory of hypertrophy. *Sci Rep* 2018;**8**:1898.
  33. Sharples AP, Stewart CE, Seaborne RA. Does skeletal muscle have an ‘epi-memory’? The role of epigenetics in nutritional programming, metabolic disease, aging and exercise. *Aging Cell* 2016;**15**:603–616.
  34. Turner DC, Seaborne RA, Sharples AP. Comparative transcriptome and methylome analysis in human skeletal muscle anabolism, hypertrophy and epigenetic memory. *Sci Rep* 2019;**9**:1–12.
  35. Sailani MR, Halling JF, Møller HD, Lee H, Plomgaard P, Pilegaard H, et al. Lifelong physical activity is associated with promoter hypomethylation of genes involved in metabolism, myogenesis, contractile properties and oxidative stress resistance in aged human skeletal muscle. *Sci Rep* 2019;**9**:1–11.
  36. Shah S, Bonder MJ, Marioni RE, Zhu Z, McRae AF, Zernakova A, et al. Improving phenotypic prediction by combining genetic and epigenetic associations. *Am J Hum Genet* 2015;**97**:75–85.
  37. Dogan MV, Grumbach IM, Michaelson JJ, Philibert RA. Integrated genetic and epigenetic prediction of coronary heart disease in the Framingham Heart Study. *PLoS One* 2018;**13**:1–18.
  38. He L, Khanal P, Morse CI, Williams A, Thomis M. Differentially methylated gene patterns between age-matched sarcopenic and non-sarcopenic women. *J Cachexia Sarcopenia Muscle* 2019;jcsm.12478.
  39. Janssen I, Baumgartner RN, Ross R, Rosenberg IH, Roubenoff R. Skeletal muscle cutpoints associated with elevated physical disability risk in older men and women. *Am J Epidemiol* 2004;**159**:413–421.
  40. Aryee MJ, Jaffe AE, Corrada-Bravo H, Ladd-Acosta C, Feinberg AP, Hansen KD, et al. Minfi: a flexible and comprehensive Bioconductor package for the analysis of Infinium DNA methylation microarrays. *Bioinformatics* 2014;**30**:1363–1369.
  41. Pidsley R, Zotenko E, Peters TJ, Lawrence MG, Risbridger GP, Molloy P, et al. Critical evaluation of the Illumina MethylationEPIC BeadChip microarray for whole-genome DNA methylation profiling. *Genome Biol* 2016;**17**:208.
  42. Ogasawara R, Thiebaud RS, Loenneke JP, Loftin M, Abe T. Time course for arm and chest muscle thickness changes following

- bench press training. *Interv Med Appl Sci* 2012;**4**:217–220.
43. Reeves ND, Maganaris CN, Narici MV. Ultrasonographic assessment of human skeletal muscle size. *Eur J Appl Physiol* 2004;**91**:116–118.
  44. Tibshirani R. Regression shrinkage and selection via the lasso. *J R Stat Soc Ser B* 1996;**58**:267–288.
  45. Akaike H. A new look at the statistical model identification. *IEEE Trans Automat Contr* 1974;**19**:716–723.
  46. Burnham KP, Anderson DR. Multimodel inference. *Sociol Methods Res* 2004;**33**:261–304.
  47. Bell JT, Tsai P, Yang T, Pidsley R, Nisbet J, Glass D, et al. Epigenome-wide scans identify differentially methylated regions for age and age-related phenotypes in a healthy ageing population. *PLoS Genet* 2012;**8**:e1002629.
  48. Singh P, James RS, Mee CJ, Morozov IY. mRNA levels are buffered upon knockdown of RNA decay and translation factors via adjustment of transcription rates in human HepG2 cells. *RNA Biol* 2019;**0**:1–9.
  49. Shekhar A, Lin X, Liu F, Zhang J, Mo H, Bastarache L, et al. Transcription factor ETV1 is essential for rapid conduction in the heart. *J Clin Invest* 2016;**126**:4444–4459.
  50. Arber S, Ladle DR, Lin JH, Frank E, Jessell TM. ETS gene Er81 controls the formation of functional connections between group Ia sensory afferents and motor neurons. *Cell* 2000;**101**:485–498.
  51. Bai SW, Herrera-Abreu MT, Rohn JL, Racine V, Tajadura V, Suryavanshi N, et al. Identification and characterization of a set of conserved and new regulators of cytoskeletal organization, cell morphology and migration. *BMC Biol* 2011;**9**:54.
  52. Cedar H, Bergman Y. Linking DNA methylation and histone modification: patterns and paradigms. *Nat Rev Genet* 2009;**10**:295–304.
  53. Charlier R, Caspers M, Knaeps S, Mertens E, Lambrechts D, Lefevre J, et al. Limited potential of genetic predisposition scores to predict muscle mass and strength performance in Flemish Caucasians between 19 and 73 years of age. *Physiol Genomics* 2017;**49**:160–166.
  54. Tiainen K, Sipilä S, Alen M, Heikkinen E, Kaprio J, Koskenvuo M, et al. Heritability of maximal isometric muscle strength in older female twins. *J Appl Physiol* 2004;**96**:173–180.
  55. Tiainen K, Sipilä S, Kauppinen M, Kaprio J, Rantanen T. Genetic and environmental effects on isometric muscle strength and leg extensor power followed up for three years among older female twins. *J Appl Physiol* 2009;**106**:1604–1610.
  56. Pasquin S, Sharma M, Gauchat JF. Ciliary neurotrophic factor (CNTF): new facets of an old molecule for treating neurodegenerative and metabolic syndrome pathologies. *Cytokine Growth Factor Rev* 2015;**26**:507–515.
  57. Roth SM, Schrage MA, Ferrell RE, Riechman SE, Metter EJ, Lynch NA, et al. CNTF genotype is associated with muscular strength and quality in humans across the adult age span. *J Appl Physiol* 2001;**90**:1205–1210.
  58. Lökk K, Modhukur V, Rajashekar B, Märtens K, Mägi R, Kolde R, et al. DNA methylome profiling of human tissues identifies global and tissue-specific methylation patterns. *Genome Biol* 2014;**15**:3248.
  59. von Haehling S, Morley JE, Coats AJS, Anker SD. Ethical guidelines for publishing in the journal of cachexia, sarcopenia and muscle: update 2019. *J Cachexia Sarcopenia Muscle* 2019;**10**:1143–1145.